Oncostatin M Expression Is Functionally Connected to Neutrophils in the Early Inflammatory Phase of Skin Repair: Implications for Normal and Diabetes-Impaired Wounds

Itamar Goren[1], Heiko Kämpfer[1], Elke Müller[1], Dana Schiefelbein[1], Josef Pfeilschifter[1] and Stefan Frank[1]

In this study, we investigated the role of the cytokine oncostatin M (OSM) for wound biology. OSM and its specific OSM receptor subunit β (OSMRβ) were induced upon injury. OSM induction paralleled the early influx of polymorphonuclear neutrophils (PMN) into the wound. OSM protein was localized in PMN in very early wounds, whereas OSMRβ could be detected on macrophages, keratinocytes, and fibroblasts later in repair. To establish a functional connection between PMN and OSM expression in wounds, we depleted mice from circulating PMN by injecting an anti-PMN monoclonal antibody (Ly-6G). PMN-depleted wounds were characterized by a nearly complete loss of OSM but not OSMRβ mRNA and protein expression within the initial 16–24 hours after injury. PMN-rich chronic wounds from diabetic *ob/ob* mice were characterized by a strongly elevated OSM mRNA and protein expression as compared to healthy animals. Moreover, a leptin-mediated improvement of chronic wounds in *ob/ob* mice was paralleled by a complete inhibition of PMN influx associated again with a dramatic loss of OSM expression at the wound site. These data constitute strong evidence that OSM expression during wound inflammation is functionally connected to PMN infiltration.

Journal of Investigative Dermatology (2006) **126,** 628–637. doi:10.1038/sj.jid.5700136; published online 12 January 2006

INTRODUCTION

Skin repair represents a highly dynamic process involving fibroplasia, angiogenesis, and neo-epithelialization paralleled by a tightly controlled gene expression at the wound site. Especially wound inflammation is established to initiate and drive skin regeneration (Martin, 1997; Singer and Clark, 1999; Werner and Grose, 2004). However, the importance of wound inflammation is double-faced. Chronic wound situations in humans and mice are associated with conditions of prolonged and dysregulated inflammation (Rosner *et al.*, 1995; Loots *et al.*, 1998; Wetzler *et al.*, 2000; Goren *et al.*, 2003). Therefore, deeper insights into underlying mechanisms with respect to wound inflammatory processes are pivotal to the future understanding of disturbed healing conditons (Jeffcoate and Harding, 2003).

[1]*pharmazentrum frankfurt/ZAFES, Klinikum der Johann Wolfgang Goethe-Universität, Frankfurt am Main, Germany*

Correspondence: Dr Stefan Frank, pharmazentrum frankfurt/ZAFES, Institut für Allgemeine Pharmakologie und Toxikologie, Klinikum der JW Goethe-Universität Frankfurt/M., Theodor-Stern-Kai 7, D-60590 Frankfurt/M., Germany. E-mail: S.Frank@em.uni-frankfurt.de

Abbreviations: LIF, leukemia inhibitory factor; Mϕ, macrophage; OSM, oncostatin M; OSMRβ, OSM receptor subunit β; PMN, polymorphonuclear neutrophils; TNF, tumor necrosis factor; PBS, phosphate-buffered saline; GAPDH, glyceraldehyde-3-phosphate dehydrogenase; SD, standard deviation

Received 25 July 2005; revised 11 November 2005; accepted 21 November 2005; published online 12 January 2006

Here, we have identified a dysregulated expression of oncostatin M (OSM) in chronic wounds of diabetic mice. OSM represents a multifunctional 28 kDa cytokine that belongs to the IL-6 family of proteins (Tanaka and Miyajima, 2003) and is produced from activated T- and monocytic cell types (Zarling *et al.*, 1986; Brown *et al.*, 1987; Malik *et al.*, 1989; Wallace *et al.*, 1999). Additionally, also polymorphonuclear neutrophils (PMN) have been recently described to be potent cellular sources of OSM biosynthesis and release under inflammatory conditions (Grenier *et al.*, 1999; Hurst *et al.*, 2002). OSM participates in growth regulation, differentiation, gene expression, and cell survival in a variety of cell types and, remarkably, also contributes to inflammation and tissue remodeling processes (Tanaka and Miyajima, 2003).

Biologic activities of OSM are mediated through binding to its specific OSM receptor subunit β (OSMRβ), which belongs to the signal transducing receptors for IL-6 type cytokines (Heinrich *et al.*, 2003). Cloning and expression of the OSMRβ revealed that OSM restrictively transduces signals through its specific receptor complex composed of gp130 and OSMRβ (Mosley *et al.*, 1996; Lindberg *et al.*, 1998; Tanaka *et al.*, 1999). The OSMRβ subunit is widely expressed in various cell types and tissues, including epithelial cells, fibroblasts, and skin tissue (Mosley *et al.*, 1996). It is important to note that its specific ligand OSM exerts potential functions in the skin, as this cytokine

stimulates mitogenic responses of dermal fibroblasts, dermal endothelial cells (Vasse *et al.*, 1999; Ihn and Tamaki, 2000) and extravasation of PMN into skin tissue after subcutaneous application (Modur *et al.*, 1997).

Here, we report evidence for a functional coupling of OSM to PMN infiltration in very early wounds. Moreover, we demonstrate that a leptin-improved healing of chronic wounds was associated with a dramatic loss of PMN cell numbers and OSM expression at the wound site. Thus, this study provides evidence that dysregulated OSM expression is functionally connected to the PMN wound infiltrate and associated with impaired healing conditions in chronically inflamed wounds.

RESULTS

OSM and OSMRβ expression in normal skin repair

OSM has been shown to be produced by inflammatory cell types such as monocytes and PMN under inflammatory conditions (Malik *et al.*, 1989; Wallace *et al.*, 1999; Grenier *et al.*, 1999; Hurst *et al.*, 2002). As wound inflammation represents a pivotal process for skin regeneration (Martin, 1997), we first determined expression of OSM and its specific receptor subunit OSMRβ in undisturbed skin repair. As shown in Figure 1a, OSM mRNA levels were induced upon injury. The very rapid increase of OSM mRNA levels in early repair was dramatic as compared to the observed low-level expression in non-wounded skin (35.2 ± 3.1-fold; $P<0.05$ as compared to control skin). Accordingly, OSM protein

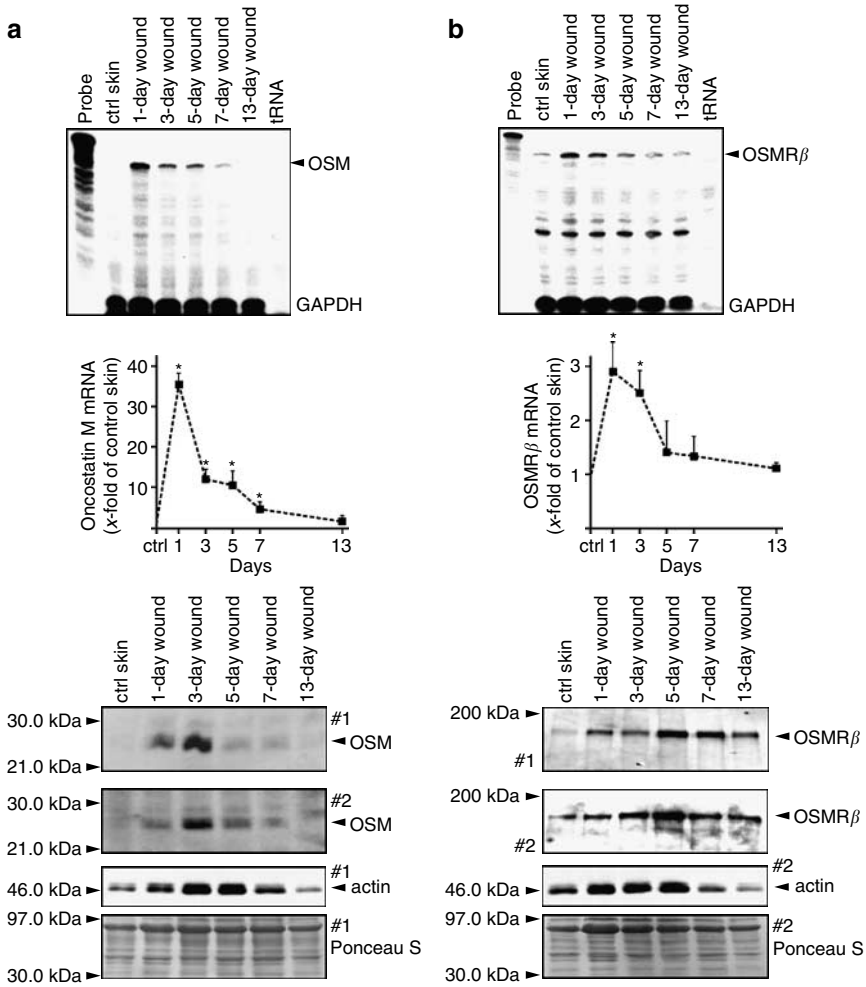

Figure 1. Expression of OSM and its OSMRβ in skin repair. Regulation of (**a**) OSM and (**b**) OSMRβ mRNA (upper panels) and protein (lower panels) expression in C57 Bl/6 mice as assessed using the RNase protection assay or immunoblot. The time after injury is indicated at the top of each lane. Ctrl skin refers to back skin biopsies of non-wounded mice. 1,000 cpm of the hybridization probe were added to the lane labeled probe. Additional bands in the probe lane represent truncated RNA transcripts. A quantification of OSM and OSMRβ mRNA (*x*-fold of control skin) is shown in the middle panels. *$P<0.05$ (analysis of variance, Dunnett's method) as compared to control skin. Bars indicate the mean $\pm$ SD obtained from wounds ($n=48$) isolated from animals ($n=12$) from three independent animal experiments. For immunoblot analysis, each time point depicts eight wounds ($n=8$) from four individual mice ($n=4$). Two independent experimental animal series (#1, #2) are shown. Loading of immunoblots and protein integrity was controlled using actin immunodetection or Ponceau S staining as indicated. Here, it is important that the observed increase in actin expression after wounding is always observed in the dynamic process of skin repair and is not because of unequal loading of the analyzed wound lysates.

expression was hardly detectable in non-wounded skin. However, wounding induced the induction of OSM protein, which appeared in marked amounts especially during early wound inflammation (days 1 and 3 post-wounding) (Figure 1a, lower panels). To complement the data on OSM expression, we also determined the regulation of its specific receptor at the wound site. Although the overall changes in mRNA and protein expression were only moderate compared to OSM regulation, we observed a clear induction of OSMRβ mRNA (2.9 ± 0.6-fold; $P < 0.05$ as compared to control skin) (Figure 1b, upper panels) and protein (Figure 1b, lower panels) expression upon injury. Induction of OSMRβ occurred rapidly after wounding, but by contrast to OSM, the increase in OSMRβ protein persisted into later stages of repair (Figure 1b, lower panels). Here, it is important to note that RNase protection assay detected an additional specific band which must represent a splice variant of the published OSMRβ transcript. Interestingly, the truncated mRNA transcript occurred to be constitutively present during repair (Figure 1b, upper panel). The observed molecular weight of approximately 180 kDa for the OSMRβ subunit in SDS-PAGE was in good accordance to three reports showing the cloning and expression of the protein (Mosley *et al.*, 1996; Lindberg *et al.*, 1998; Tanaka *et al.*, 1999).

Localization of OSM and its OSMRβ subunit at the wound site

As a next step, we determined the cellular sources of OSM and OSMRβ expression during repair. Double staining of wound serial sections showed that early wound tissue (24 hours after injury) was characterized by OSM expressing PMN (Figure 2a–c). During a later stage of healing (day 3 post-wounding), we observed that OSM was not only expressed in PMN, as a different nuclear morphology identified also a macrophage (Mϕ) subset of infiltrating immune cells to express OSM at the wound site (Figure 2e). In line with the disappearance of OSM at later stages of repair (Figure 1a), we could detect only a few OSM-positive cells within the granulation tissue of 5-day wounds (Figure 2f). However, immunohistochemistry suggested also wound margin keratinocytes as potential producers of OSM (Figure 2f and g), which might contribute to the overall decreasing and weak expression of OSM at that stage of repair (Figure 1a, lower panels). We performed a pre-incubation of the anti-OSM antiserum with recombinant murine OSM protein before immunohistochemistry to block and thus control specific antibody binding to OSM antigens in tissue sections (Figure 2d and h).

OSMRβ localization at the wound site appeared to be diverse. We detected OSMRβ to be expressed in a subset of infiltrating immune cells in early (3 days) and later healing (7 days). Owing to nuclear morphology, these OSMRβ-positive cells were most likely Mϕ rather than the PMN cell type of the infiltrate (Figure 3a, e, g and h). Moreover, the absence of PMN, which have disappeared from the wound at this stage of repair in undisturbed 7-day wounds (Wetzler *et al.*, 2000), again strongly argued for OSMRβ-expressing Mϕ. Additionally, we could also observe fibroblasts (Figure 3b) and keratinocytes (Figure 3c and d) to express OSMRβ during repair. An unspecific goat IgG incubation (Figure 3f) served as negative control.

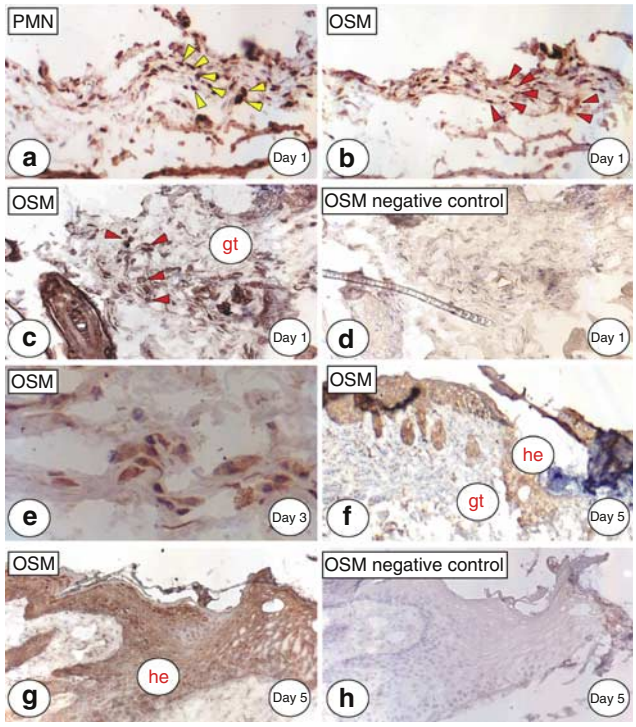

Figure 2. Localization of OSM protein in regenerating skin. Frozen serial sections from mouse wounds (days 1, 3, and 5 post-wounding) were incubated with a polyclonal goat antiserum directed against murine OSM or with a monoclonal antibody against PMN-specific Ly-6G as indicated. All sections were stained with the avidin–biotin–peroxidase complex system using 3,3-diaminobenzidine-tetrahydrochloride as a chromogenic substrate. Nuclei were counterstained with hematoxylin. Immunopositive signals within the sections are indicated with arrows. Specificity of the anti-OSM antiserum (OSM negative control) was controlled by pre-adsorption of the antiserum using a recombinant OSM protein. gt, granulation tissue; he, hyperproliferative epithelium.

OSM is preferentially expressed in inner wound areas (granulation tissue)

To strengthen the histologic data concerning the cellular sources of OSM expression, we now analyzed the expression of OSM in distinct compartments of wound tissue (Figure 4a). Tissue was taken from 3-day wounds and divided into ''wound margin'' tissue (which contained part of the non-wounded epidermis and dermis, and, more importantly, the complete developing wound margin epithelia) and the ''inner wound'' (which contained the complete developing granulation tissue consisting of PMN, Mϕ, fibroblasts, and endothelial cells). We found OSM mRNA (Figure 4b) and protein (Figure 4c) to be predominantly expressed in the inner wound compartment (inner wound 443 ± 139 Phospholmager photostimulated luminescence (PSL) counts versus 131 ± 5.3 PSL counts in wound margins, $P < 0.05$). This result was in good accordance to our observation of OSM-expressing immune cells (Figure 2), which are predominantly localized within the granulation tissue. A recombinant 21.0 kDa truncated murine

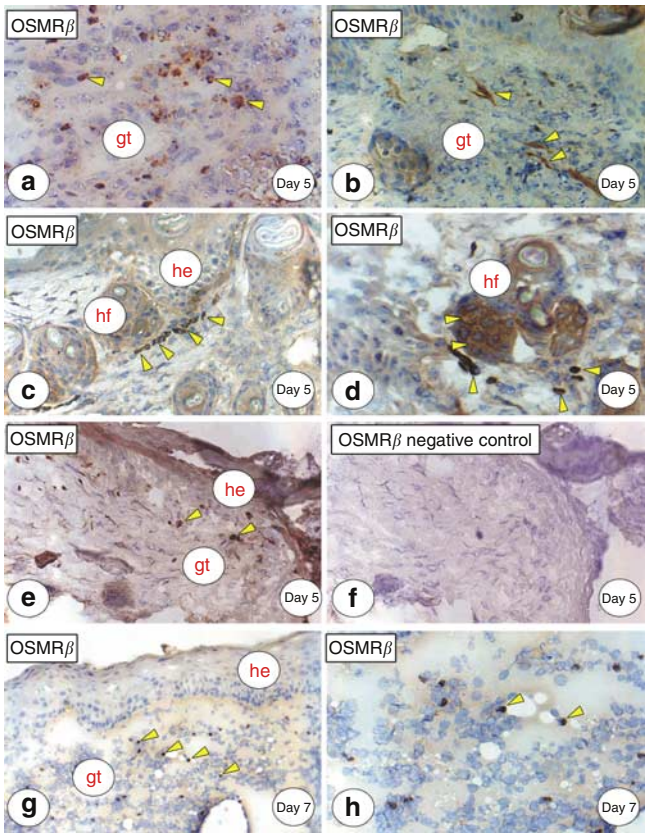

Figure 3. Localization of OSMRβ protein in regenerating skin. Frozen serial sections from mouse wounds (days 3, 5, and 7 post-wounding) were incubated with polyclonal goat antiserum directed against murine OSMRβ as indicated. All sections were stained with the avidin–biotin–peroxidase complex system using 3,3-diaminobenzidine-tetrahydrochloride as a chromogenic substrate. Nuclei were counterstained with hematoxylin. Immunopositive signals within the sections are indicated with arrows. Specificity of the goat anti-OSMRβ antiserum (OSMRβ negative control) was controlled by incubation of the tissue section using an unspecific goat IgG. gt, granulation tissue; he, hyperproliferative epithelium; hf, hair follicle.

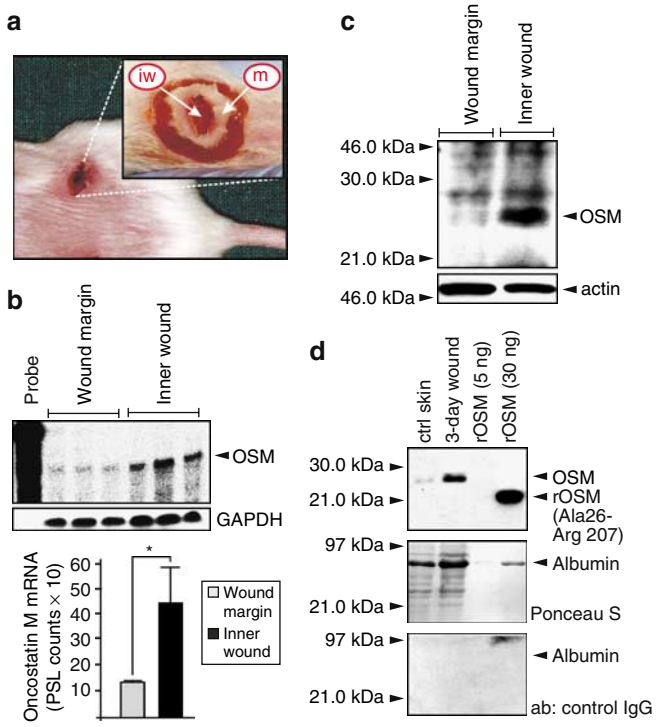

Figure 4. Spatial distribution of OSM expression in wound tissue. (**a**) Overview to show tissue sampling for inner wound (iw) and wound margin (m). (**b**) OSM mRNA and (**c**) protein expression in 3-day wound margin and inner wound isolated from C57 Bl/6 wild-type mice assessed using the RNase protection assay or immunoblot. (**b**) For mRNA expression, we have analyzed one wound each isolated from three individual animals ($n=3$) per independent experimental series. Every data point depicts the OSM-specific signal from three wound compartments isolated from three individual mice ($n=3$) which have been pooled before analysis. Bars (mean ± SD) indicate data obtained from three independent animal experiments ($n=3$) that have been used for statistical analysis. $^*P<0.05$ as indicated by the bracket. For immunoblot analysis, each time point depicts isolated wound compartments of six wounds ($n=6$) from three individual mice ($n=3$). Immunodetection of actin was used to control equal loading. (**d**) Specificity of the used anti-OSM antiserum was confirmed using a 21 kDa truncated recombinant murine OSM protein (rOSM) (middle panel) and by re-probing the same immunoblot using a normal IgG in combination with the same secondary antibody (lower panels).

OSM protein and an unspecific control IgG was used to control the specificity of the anti-OSM antiserum (Figure 4d, lower panel).

Depletion of early wound tissue from PMN severely inhibited expression of proinflammatory cytokines and OSM at the wound site

As we had identified PMN as producers of OSM in initial wound healing, we now tried to prove a direct functional connection between OSM expression and early PMN influx in early wound repair. To do so, we treated healthy mice by systemic injection of the rat monoclonal antibody Ly-6G (1 μg/g body weight, once a day) two days before wounding. This antibody specifically recognizes the GR-1 epitope on murine PMN and has been described to cause a long-lasting neutropenia when injected into mice (Thakur *et al.*, 1996). First, we controlled the neutropenic efficiency of treatment. Neutropenic treatment of mice with the anti-Ly-6G antibody was very efficient, as we could not detect any PMN-specific signals in early wound tissue (Figure 5a, upper panel). Using immunoblot analysis, we observed infiltrating Mϕ (as assessed by the Mϕ-specific F4/80 antibody) after 16 and 24 hours under both conditions of treatment (Figure 5a, lower panel). However, it is important to note that immunoblotting using the F4/80 antibody appeared to be limited with respect to sensitivity. Thus, we have alternatively determined lysozyme M mRNA expression, which is known to be constitutively expressed in Mϕ and can be used to determine the presence of this cell type in wound tissue (Wetzler *et al.*, 2000; Goren *et al.*, 2003). As shown in Figure 5b, we could indeed detect the presence of tissue Mϕ in non-wounded control skin. Wounding induced a slow and moderate increase in Mϕ numbers as compared to 3-day wounds, which are characterized by highest Mϕ cell numbers in skin repair (diPietro, 1995; Wetzler *et al.*, 2000; Goren *et al.*,

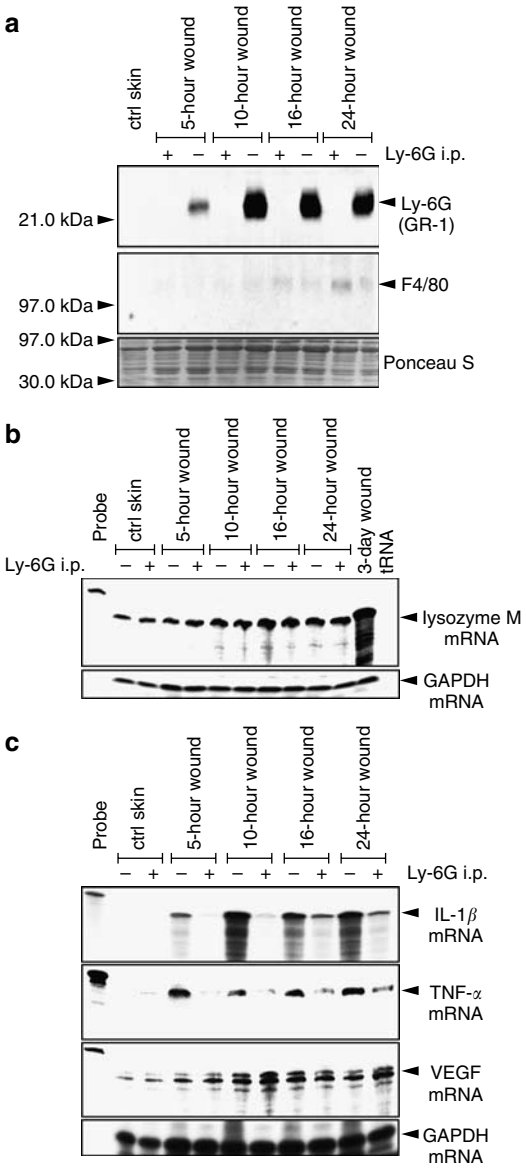

Figure 5. Systemic treatment of mice with an anti-Ly-6G antibody depletes wound tissue from PMN and cytokine expression. (**a**) Immunoblots showing the presence of PMN (upper panels, as assessed by Ly-6G) or Mϕ (as assessed by F4/80) in wounds of Ly-6G-induced neutropenic or mock-treated control mice as indicated. For immunoblot analysis, each time point depicts eight wounds ($n=8$) from four individual mice ($n=4$). Loading of immunoblots and protein integrity was controlled using a Ponceau S staining. Regulation of (**b**) lysozyme M, or (**c**) IL-1β, TNF-α, vascular endothelial growth factor, and GAPDH mRNA expression in wounds of Ly-6G-induced neutropenic or mock-treated control mice as indicated. The time after injury is given at the top of each lane. Ctrl skin refers to back skin biopsies of non-wounded mice. One thousand cpm of the hybridization probe were added to the lane labeled probe.

2003). Not unexpected, however, we did not observe an effect of the Ly-6G antibody on the presence of Mϕ in early wounds (Figure 5b).

As PMN have been established as the first producers of proinflammatory cytokines within the first 24 hours at the wound site (Hübner *et al.*, 1996), we additionally determined mRNA expression for IL-1β and tumor necrosis factor (TNF) α as indicated. Transcripts of both cytokines were downregulated in PMN-depleted wound conditions (Figure 5c, upper panels) suggesting that infiltrating PMN might be functionally connected to an early cytokine expression following injury in the presence of unchanged vascular endothelial growth factor and glyceraldehyde-3-phosphate dehydrogenase (GAPDH) mRNA levels (Figure 5b, lower panels).

In line with the effects of PMN depletion on cytokine expression, we found also OSM expression to be dependent on early PMN infiltration (Figure 6). We observed a marked downregulation of OSM mRNA (phosphate-buffered saline (PBS)-treated 168 ± 73 PSL counts versus Ly-6G 39 ± 19 PSL counts, $P<0.05$) (Figure 6a) and OSM protein (Figure 6b) expression in very early wounds of Ly-6G-treated mice. Remarkably, PMN-mediated differences in OSM protein levels diminished after 24 hours (Figure 6b, 24 hours *wound*), here suggesting that the re-appearance of OSM protein at this time point of healing might be linked to Mϕ (Figure 5a and b), which have been shown to express OSM (Figure 2e). Interestingly, expression of the OSM-specific OSMRβ subunit mRNA (PBS-treated 165 ± 36 PSL counts versus Ly-6G 156 ± 18 PSL counts) (Figure 7a) and protein (Figure 7b) was not changed under the same experimental conditions in PMN-depleted wounds. A normal goat IgG control revealed the specificity of the anti-OSMRβ immunoblot (data not shown).

Improved healing of chronic wounds in diabetic *ob/ob* mice is associated with a dramatic downregulation of OSM expression and PMN influx

Finally, we investigated the expression of OSM during skin repair in *ob/ob* mice. *Ob/ob* animals are characterized by a type II diabetes (Coleman, 1978) and develop severely impaired wound healing conditions after injury (Frank *et al.*, 2000) associated with highly elevated numbers of PMN and Mϕ (Goren *et al.*, 2003). As shown in Figure 8a, fully developed 13-day chronic wounds in *ob/ob* mice were clearly characterized by markedly elevated levels of OSM mRNA (for OSM mRNA in 13-day wounds in control mice refer to Figure 1a) and protein as compared to healthy C57 Bl/6 animals. As a next step, we treated *ob/ob* mice with recombinant leptin (2 μg/g body weight/day) during the healing period. Here, it is important to note that a distinct difference in PMN infiltrate between diabetes-impaired and leptin-improved healing in *ob/ob* mice is restricted to the late healing time point (day 13 post-wounding) (Goren *et al.*, 2003). Accordingly, leptin treatment markedly downregulated elevated OSM mRNA (PBS-treated 191 ± 46 PSL counts versus leptin 52 ± 20 PSL counts, $P<0.01$) and protein levels during improved repair in late 13-day wounds (Figure 8b). In good accordance to the observed functional coupling between wound PMN and OSM levels, we determined the complete absence of infiltrating PMN in the presence of again dramatically reduced OSM levels (Figure 8c, left panels). Interestingly, PMN can be located in complete wound tissue including the wound scab (Figure 8d). Moreover,

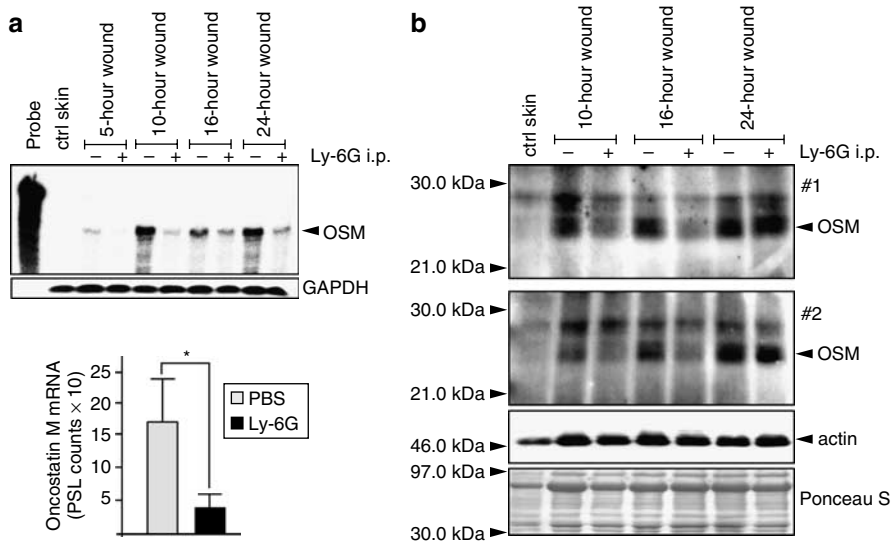

Figure 6. Wounds of neutropenic mice are characterized by strongly reduced OSM levels. (**a**) Regulation of OSM mRNA expression in wounds of Ly-6G-induced neutropenic or mock-treated control mice as indicated. The time after injury is given at the top of each lane. Ctrl skin refers to back skin biopsies of non-wounded mice. One thousand cpm of the hybridization probe were added to the lane labeled probe. Hybridization against GAPDH is shown as a loading control. A quantification of OSM mRNA is shown in the lower panel. $^*P<0.05$ as indicated by the bracket. Bars indicate the mean $\pm$ SD obtained from wounds ($n=9$) isolated from three animals ($n=3$). (**b**) Immunoblots showing the expression of OSM in wounds of Ly-6G-induced neutropenic or mock-treated control mice as indicated. For immunoblot analysis, each time point depicts eight wounds ($n=8$) from four individual mice ($n=4$). Two independent animal experiments (#1, #2) are shown. Loading of immunoblots and protein integrity was controlled using actin immunodetection or Ponceau S staining as indicated. Here, it is important that the observed increase in actin expression after wounding is always observed in the dynamic process of skin repair and is not because of unequal loading of the analyzed wound lysates.

leptin-mediated changes in OSM expression were most likely independent from Mϕ in diabetic wounds, as leptin-mediated OSM changes occurred in the presence of an unaltered infiltration of Mϕ (Figure 8c, right panels). Finally, we did not observe an overall change in OSMRβ mRNA expression in chronic versus leptin-improved repair at day 13 post-wounding (PBS-treated 131 $\pm$ 28 PSL counts versus leptin 136 $\pm$ 20 PSL counts, not significant) (Figure 8e). However, the kinetics of OSMRβ protein expression during impaired healing was clearly different to that observed in normal skin repair (Figure 8f; for normal repair, refer to Figure 1b).

DISCUSSION

Diabetic ulcerations represent severely disturbed healing conditions in injured skin tissue that are associated with a dramatically exacerbated and prolonged inflammation at the wound site (Rosner *et al.*, 1995; Loots *et al.*, 1998; Wetzler *et al.*, 2000; Goren *et al.*, 2003). Within this context, it was quite remarkable to identify OSM as a potentially dysregulated factor from inflamed, chronic wound tissue which has been isolated from diabetic *ob/ob* mice. OSM is now suggested to participate in dynamic processes such as growth regulation, differentiation, inflammation, and tissue remodeling (Tanaka and Miyajima, 2003). OSM has been described to inhibit the growth of carcinoma cell lines (Brown *et al.*, 1987). Therefore, it is tempting to speculate that appearance of OSM within the initial 48 hours of repair might function to inhibit early keratinocyte proliferation, which is delayed after injury to allow the cells to migrate into the area of injury (Clark, 1996). In line, we observed a disappearing OSM in overlap with the development of the massive wound margin epithelia (Singer and Clark, 1999). A second line of evidence supports an additional role of OSM in wound biology. OSM has been shown to serve as a potent mitogen for isolated human dermal fibroblasts and human dermal microvasculature endothelial cells (Vasse *et al.*, 1999; Ihn and Tamaki, 2000) and to induce vascular endothelial growth factor in smooth muscle or monocytic cell types (Repovic *et al.*, 2003; Faffe *et al.*, 2005). In line with these reports, we found OSM to be expressed in inner wound areas, exactly where fibroplasia and neo-vascularization takes place. In accordance, this observation suggests that the observed increase in OSM in late disturbed wound tissue might be an adaptive regulatory process to compensate for the reduced mitogenic responses of wound fibroblasts and endothelial cells.

Three major cell types are established as producers of OSM under different conditions *in vitro* and *in vivo*: activated T lymphocytes (Brown *et al.*, 1987), activated monocytic cells (Zarling *et al.*, 1986; Wallace *et al.*, 1999), and PMN (Grenier *et al.*, 1999; Hurst *et al.*, 2002). In good accordance, we could actually immunolocalize PMN and Mϕ, respectively, in the very initial and early phases of wound inflammation using an OSM-specific antiserum. PMN represent the very first immune cells, infiltrating within minutes into the area of injury (Martin, 1997; Singer and Clark, 1999). We could confirm the very early appearance of this cell type in our study, as we observed a very prominent and pronounced PMN-specific signal in wound lysates 5 hours

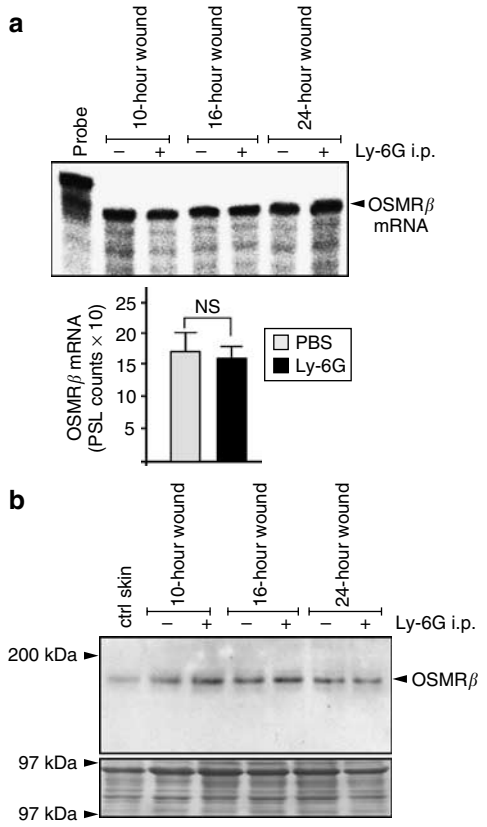

Figure 7. OSMRβ expression is not dependent on PMN influx in early wounds. (**a**) Regulation of OSMRβ mRNA expression in wounds of Ly-6G-induced neutropenic or mock-treated control mice as indicated. The time after injury is given at the top of each lane. One thousand cpm of the hybridization probe were added to the lane labeled probe. A quantification of OSMRβ mRNA is shown in the lower panel. NS, not significant as indicated by the bracket. Bars indicate the mean ± SD obtained from wounds ($n = 9$) isolated from three animals ($n = 3$). (**b**) Immunoblot showing the expression of OSMRβ in wounds of Ly-6G-induced neutropenic or mock-treated control mice as indicated. For immunoblot analysis, each time point depicts eight wounds ($n = 8$) from four individual mice ($n = 4$). One representative experiment is shown. Loading of immunoblots and protein integrity was controlled using Ponceau S staining.

following injury. With respect to published data, we hypothesized that the rapid increase in wound OSM levels might be connected, at least partially, to the early PMN wound infiltrate, as PMN have been described to carry intracellular stores of biologically active OSM (Grenier *et al.*, 1999). Interestingly, we could observe a nearly complete loss of OSM protein in PMN-depleted early wounds from neutropenic mice after injection of the anti-PMN antibody Ly-6G. This antibody has been convincingly demonstrated to induce severe neutropenic states in mice in a dose-dependent manner (Thakur *et al.*, 1996).

Here, it is reasonable to argue that the overall loss of OSM protein at the wound site must be a functional consequence of the missing PMN infiltrate at the early site of injury. This observation indicates an important role of this cell type in very early tissue regeneration. With respect to our data it must remain unclear, however, to what extent a direct effect on PMN-expressed and secreted OSM contributed to the observed loss of OSM in early wounds. As we had observed PMN as producers of OSM by immunohistochemistry, it now comes clear that at least a part of the observed wound-specific OSM is imported by this specific subset of immune cells into the wound site as a stored cytokine ''cargo''. By contrast, we cannot exclude that a PMN-driven OSM expression by resident wound cells might also contribute to the observed effects. Moreover, the observation that PMN express IL-1β and TNF-α in wound tissue (Hübner *et al.*, 1996) might also explain the strong attenuation of IL-1β and TNF-α in PMN-depleted early wounds, which again supports the ''cargo''-principle in PMN with respect to these cytokines. Additionally, the observed attenuation of IL-1β and TNF-α expression in PMN-depleted wound tissue implicates that the very early wound response was not augmented by an increased bacterial infection in the absence of microbicidal PMN. In good accordance with early wound conditions, we observed a decrease in OSM expression in PMN-diminished late healing wounds of leptin-treated *ob/ob* mice. Here, it is suggested that leptin might contribute to this process via its effects on wound keratinocytes, as it turns off the expression of PMN-attracting CXC-chemokines in neo-epithelia *in vivo* (Goren *et al.*, 2003).

Finally, one question still remains: what functions might be served by OSM in the control of wound inflammation? Interestingly, some properties of OSM for skin inflammation have been shown by a subcutaneous injection of human recombinant OSM into mice (Modur *et al.*, 1997). In this animal model, human OSM induced a local inflammatory response including the extravasation of PMN. Moreover, OSM was highly selective for PMN recruitment (Kerfoot *et al.*, 2001), capable to induce the endothelial transmigration of PMN via induction of different selectins, and efficient to mediate the synthesis of PMN-attracting chemokines at the site of inflammation (Modur *et al.*, 1997; Kerfoot *et al.*, 2001). However, consequences of these data have to be interpreted very carefully with respect to functional properties of OSM in cutaneous inflammation. A paper by Lindberg *et al.* (1998) convincingly showed that human OSM restrictively signaled through receptors containing the LIFRβ and gp130, but not through the mouse OSMRβ subunit. That means that the above mentioned study of human OSM actions in murine skin (Modur *et al.*, 1997) did not elucidate the biology of OSM but reflected the biological actions of LIF. Nevertheless, OSM functions have to be potentially interpreted as proinflammatory in the skin organ system. This hypothesis is further strengthened by our observation that highly inflamed diabetes-impaired wounds were clearly characterized by a marked overexpression of the cytokine OSM.

In summary, this study provides evidence that OSM contributes to wound inflammation under normal, but also impaired healing conditions. OSM expression was functionally connected to the early PMN infiltrate. Thus, our data strongly support an important role of the early PMN infiltrate in the regulation and biosynthesis of cytokines in cutaneous wound healing.

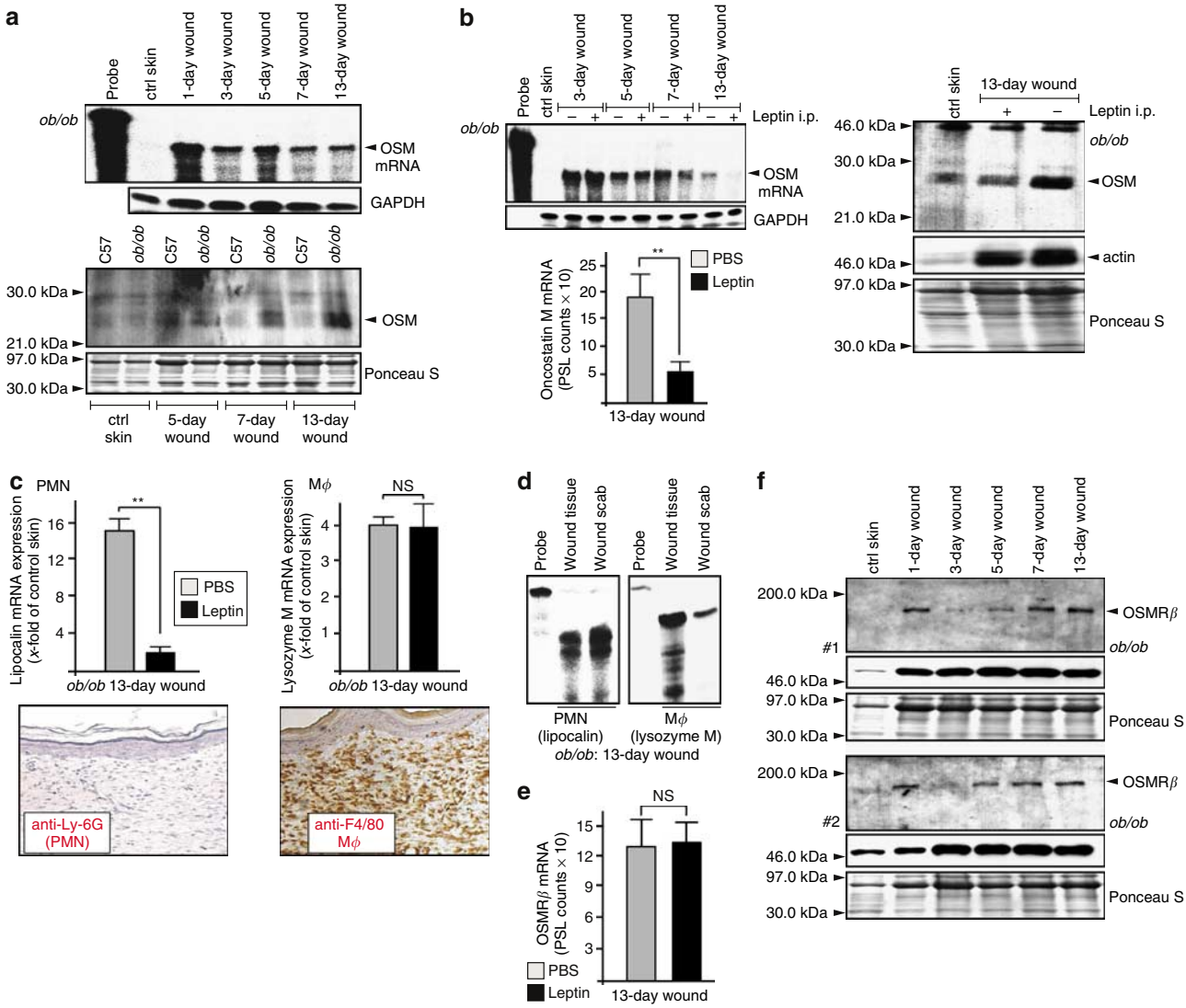

Figure 8. Diabetes-impaired repair in *ob/ob* mice is associated with dysregulated OSM and OSMRβ expression at the wound site. (**a**) Regulation of OSM mRNA (upper panel) and protein (lower panel) expression in diabetic *ob/ob* and C57 Bl/6 mice as assessed using the RNase protection assay or immunoblot. Each time point depicts 16 wounds ($n=16$) from four individual mice ($n=4$) for RNA analysis and eight wounds from four individual mice ($n=4$) for protein analysis. The time after injury is indicated. Loading of immunoblots and protein integrity was controlled using Ponceau S staining. (**b**) RNase protection assay for OSM mRNA (upper panels) in wounds of PBS- and leptin-treated mice. Each time point depicts 12 wounds ($n=12$) from four individual mice ($n=4$). Treatment and time after injury are indicated. The quantification of OSM mRNA is shown in the middle panel. $^{**}P<0.01$ as indicated by the bracket. Bars indicate the mean $\pm$ SD obtained from wounds ($n=12$) isolated from four animals ($n=4$). Immunoblot for OSM expression in 13-day wounds of PBS- and leptin-treated *ob/ob* mice is shown in the lower panel. Each time point depicts eight wounds ($n=8$) from four individual mice ($n=4$). Loading of immunoblot and protein integrity was controlled using actin immunodetection and Ponceau S staining as indicated. Here, it is important that the observed increase in actin expression after wounding is always observed in the dynamic process of skin repair and is not because of unequal loading of the analyzed wound lysates. (**c**) A quantification of lipocalin (marker for PMN) and lysozyme M (marker for Mϕ) mRNA (*x*-fold of control skin). $^{**}P<0.01$; NS, not significant as indicated by the brackets. Bars indicate the mean $\pm$ SD obtained from wounds ($n=48$) from animals ($n=12$) from three independent animal experiments. The *in situ* determination of PMN (anti Ly-6G) and Mϕ (anti-F4/80) in 13-day wounds of leptin-treated *ob/ob* mice is shown in the lower panels. (**d**) RNase protection assay demonstrating the distribution of PMN and Mϕ in the wound tissue and wound scab compartment of diabetic *ob/ob* mice. (**e**) A quantification of OSMRβ mRNA in 13-day wounds of PBS- and leptin-treated *ob/ob* mice. NS, not significant as indicated by the bracket. Bars indicate the mean $\pm$ SD obtained from wounds ($n=12$) isolated from four animals ($n=4$). (**f**) immunoblots for OSMRβ expression in wounds of diabetic *ob/ob* mice. The time after injury is indicated. Each time point depicts eight wounds ($n=8$) from four individual mice ($n=4$). Two independent animal experiments (#1, #2) are shown. Loading of immunoblots and protein integrity was controlled using actin immunodetection or Ponceau S staining as indicated. Here, it is important that the observed increase in actin expression after wounding is always observed in the dynamic process of skin repair and is not because of unequal loading of the analyzed wound lysates.

MATERIALS AND METHODS

Animals

Female C57BL/6J (wild type) and C57BL/6J-*ob/ob* mice were obtained from The Jackson Laboratories (via Charles River, Sulzfeld, Germany) and maintained under a 12 hours light/12 hours dark cycle at 22°C until they were 8 weeks of age. At this time they were caged individually, monitored for body weight, and wounded as described below.

Treatment of mice

Murine recombinant leptin (2 μg/g body weight) (Calbiochem, Bad Soden, Germany) and purified rat monoclonal anti-PMN antibody Ly-6G (Thakur *et al.*, 1996) (1 μg/g body weight) (BD Pharmingen, Heidelberg, Germany) were injected intraperitoneally in 0.5 ml PBS for the indicated time periods. Control mice were treated with PBS or an unspecific rat IgG (Santa Cruz. Heidelberg, Germany), respectively.

Wounding of mice

Wounding of mice was performed as described previously (Frank *et al.*, 1999; Stallmeyer *et al.*, 1999). Briefly, mice were anesthetized with a single intraperitoneal injection of ketamine (80 mg/kg body weight)/xylazine (10 mg/kg body weight). The hair on the back of each mouse was cut, and the back was subsequently wiped with 70% ethanol. Six full-thickness wounds (5 mm in diameter, 3–4 mm apart) were made on the back of each mouse by excising the skin and the underlying *panniculus carnosus*. The wounds were allowed to form a scab. Skin biopsy specimens were obtained from the animals 1, 3, 5, 7, 10, and 13 days after injury. At each time point, an area which included the scab and the complete epithelial margin was excised from each individual wound. The scab was included for analysis as it covers immune cells and bioactive mediators (Goren *et al.*, 2003). As a control, a similar amount of skin was taken from the backs of non-wounded mice. For each experimental time point of every individual animal experiment, tissue from four wounds each from four animals ($n=16$ wounds, RNA analysis) and from two wounds each from four animals ($n=8$ wounds, protein analysis) were combined and used for RNA and protein preparation. Pooling of wound samples guarantees the experimental basis to determine a consistent and reliable expression pattern for genes and proteins of interest between different individual animal experiments. Non-wounded back skin from four animals served as a control. Data from at least three individual animal experiments were used to perform the statistical evaluations. All animal experiments were carried out according to the Declaration of Helsinki Principles and with the permission from the local government of Hessen (Germany).

RNA isolation and RNase protection analysis

RNA isolation and RNase protection assays were carried out as described previously (Chomczynski and Sacchi, 1987; Frank *et al.*, 1999). Briefly, 20 μg of total RNA from wounded or non-wounded skin was used for RNase protection assay. DNA probes were cloned into the transcription vector pBluescript II KS(+)(Stratagene, Heidelberg, Germany) and linearized. An antisense transcript was synthesized *in vitro* using T3 or T7 RNA polymerase and [α-^{32}P]UTP (800 Ci/mmol). RNA samples were hybridized at 42°C overnight with 100.000 cpm of the labeled antisense transcript. Please note that we always used cocktails of labeled antisense transcripts: the probes of interest and the GAPDH equilibration antisense transcipts were simultaneously hybridized in the same sets of total RNA in all presented RNase protection assays. Hybrids were digested with RNases A and T1 for 1 hour at 30°C. Under these conditions, every single mismatch is recognized by the RNases. Protected fragments were separated on 5% acrylamide/8 M urea gels and analyzed using a PhosphoImager (Fuji, Straubenhardt, Germany). Subsequently, the probe of interest and the GAPDH equilibration marker were separated on the same gel for each individual experimental approach that allows for a direct and reliable loading control in all experiments. RNases A and T1 were from Roche Biochemicals (Mannheim, Germany). The murine cDNA probes were cloned using reverse transcription-PCR. The probes corresponded to nt 303–546 (for OSM, Acc. No. D31942), nt 389–645 (for OSMRβ, Acc. No. NM011019), nt 481–739 (for IL-1β, Acc. No. NM0083461), nt 541–814 (for TNF-α, Acc. No. NM013693), nt 139–544 (for vascular endothelial growth factor, Acc. No. M95200), nt 816–1481 (for lipocalin, Acc. No. X81627), nt 425 (exon 1) to 170 (exon 2) (for lysozyme M, Acc. No. M21047), nt 796–1063 (for cyclooxygenase [COX]-2, Acc. No. M64291), or nt 163–317 (for GAPDH, Acc. No. NM002046) of the published sequences.

Immunoblot analysis

Wound tissue lysates were prepared as described previously (Kämpfer *et al.*, 1999). Briefly, skin samples were homogenized in lysis buffer (1% Triton X-100, 20 mM Tris/HCl, pH 8.0, 137 mM NaCl, 10% glycerol, 5 mM ethylenediamine tetraacetic acid, 1 mM phenylmethylsulfonyl fluoride, 5 μg/ml aprotinin, 5 μg/ml leupeptin). The extracts were cleared by centrifugation. Fifty micograms of total protein lysate was separated using SDS-gel electrophoresis and specific proteins were detected using antisera directed against OSM or OSMRβ (Santa Cruz, Heidelberg, Germany), respectively. The specificity of the anti-OSM antiserum was confirmed using a truncated murine recombinant OSM protein (21 kDa, Ala26-Arg207) (R&D Systems, Wiesbaden, Germany). A secondary antibody coupled to horseradish peroxidase and the enhanced chemiluminescence detection system was used to visualize the proteins of interest. Phenylmethylsulfonyl fluoride, aprotinin and leupeptin were from Sigma (Deisenhofen, Germany) or Roche Biochemicals (Mannheim, Germany). The enhanced chemiluminescence detection system was obtained from Amersham (Freiburg, Germany).

Immunohistochemistry

Mice were wounded as described above. Animals were killed at days 1, 3, 5, and 7 after injury. Complete wounds were isolated from the back, bisected, and frozen in tissue freezing medium. Six micron frozen sections were subsequently analyzed using immunohistochemistry as described (Stallmeyer *et al.*, 1999). Polyclonal antisera against OSM and the OSMRβ (Santa Cruz, Heidelberg, Germany) were used for immunodetection. Specificity of the goat anti-OSM antibody was controlled by a 2 hours pre-incubation of the antibody with a truncated murine recombinant OSM protein (21 kDa, Ala26-Arg207) (R&D systems, Wiesbaden, Germany) before its exposure to wound tissue sections. The pre-adsorption blocks and thus controls the specific binding of the anti-OSM antiserum. The goat anti-OSMRβ was controlled using an incubation of tissue sections with an unspecific goat IgG (Santa Cruz, Heidelberg, Germany) before incubation with the secondary antibody, as a recombinant OSMRβ protein was not available.

Statistical analysis

Data are shown as means ± standard deviation (SD). Data analysis was carried out using the unpaired Student's *t*-test with raw data. Statistical comparison between more than two groups was carried out by analysis of variance (analysis of variance, Dunnett's method).

CONFLICT OF INTEREST

The authors state no conflict of interest.

ACKNOWLEDGMENTS

We thank Dr M. Kock and Dr A. Theisen for their help with the animal experiments. This work was supported by the Deutsche Forschungsgemeinschaft (SFB 553, grant FR 1540/1-1).

REFERENCES

Brown TJ, Lioubin MN, Marquardt H (1987) Purification and characterization of cytostatic lymphokines produced by activated human T lymphocytes. Synergistic antiproliferative activity of transforming growth factor beta 1, interferon-gamma, and oncostatin M for human melanoma cells. *J Immunol* 139:2977–83

Chomczynski P, Sacchi N (1987) Single-step method of RNA isolation by acid guanidinium thiocyanate-phenol-chloroform extraction. *Anal Biochem* 162:156–9

Clark RAF (1996) Wound repair: overview and general considerations. In: *The molecular and cellular biology of wound repair* (Clark RAF, ed.), New York and London: Plenum Press, 3–50

Coleman DL (1978) Obese and diabetes: two mutant genes causing diabetes-obesity syndromes in mice. *Diabetologia* 14:141–8

DiPietro LA (1995) Wound healing: the role of the macrophage and other immune cells. *Shock* 4:233–40

Faffe DS, Flynt L, Mellema M, Whitehead TR, Bourgeois K, Panettieri RA Jr *et al.* (2005) Oncostatin M causes VEGF release from human airway smooth muscle: synergy with IL-1beta. *Am J Physiol Lung Cell Mol Physiol* 288:L1040–8

Frank S, Stallmeyer B, Kämpfer H, Kolb N, Pfeilschifter J (1999) Nitric oxide triggers enhanced induction of vascular endothelial growth factor expression in cultured keratinocytes (HaCaT) and during cutaneous wound repair. *FASEB J* 13:2002–14

Frank S, Stallmeyer B, Kämpfer H, Kolb N, Pfeilschifter J (2000) Leptin enhances wound re-epithelialization and constitutes a direct function of leptin in skin repair. *J Clin Invest* 106:501–9

Goren I, Kämpfer H, Podda M, Pfeilschifter J, Frank S (2003) Leptin and wound inflammation in diabetic *ob/ob* mice. Differential regulation of neutrophil and macrophage influx and a potential role for the scab as a sink for inflammatory cells and mediators. *Diabetes* 52:2821–32

Grenier A, Dehoux M, Boutten A, Arce-Vicioso M, Durand G, Gougerot-Pocidalo MA *et al.* (1999) Oncostatin M production and regulation by human polymorphonuclear neutrophils. *Blood* 93:1413–21

Heinrich PC, Behrmann I, Haan S, Hermanns HM, Müller-Newen G, Schaper F (2003) Principles of interleukin (IL)-6-type cytokine signalling and *ist* regulation. *Biochem J* 374:1–20

Hübner G, Brauchle M, Smola H, Madlener M, Fässler R, Werner S (1996) Differential regulation of pro-inflammatory cytokines during wound healing in normal and glucocorticoid-treated mice. *Cytokine* 8:548–56

Hurst SM, McLoughlin RM, Monslow J, Owens S, Morgan L, Fuller GM *et al.* (2002) Secretion of oncostatin M by infiltrating neutrophils: regulation of IL-6 and chemokine expression in human mesothelial cells. *J Immunol* 169:5244–51

Ihn H, Tamaki K (2000) Oncostatin M stimulates the growth of dermal fibroblasts via a mitogen-activated protein kinase-dependent pathway. *J Immunol* 165:2149–55

Jeffcoate WJ, Harding KG (2003) Diabetic foot ulcers. *Lancet* 361:1545–51

Kämpfer H, Kahlina U, Mühl H, Pfeilschifter J, Frank S (1999) Counterregulation of interleukin-18 mRNA and protein expression during cutaneous wound repair in mice. *J Invest Dermatol* 113:369–74

Kerfoot SM, Raharjo E, Ho M, Kaur J, Seriom S, McCafferty DM *et al.* (2001) Exclusive neutrophil recruitment with oncostatin M in a human system. *Am J Pathol* 159:1531–9

Lindberg RA, Juan TSC, Welcher AA, Sun Y, Cupples R, Guthrie B *et al.* (1998) Cloning and characterization of a specific receptor for mouse oncostatin M. *Mol Cell Biol* 18:3357–67

Loots MA, Lamme EN, Zeegelaar J, Mekkes JR, Bos JD, Middelloop E (1998) Differences in cellular infiltrate and extracellular matrix of chronic diabetic and venous ulcers versus acute wounds. *J Invest Dermatol* 111:850–7

Malik N, Kallestad JC, Gunderson NL, Austin SD, Neubauer MG, Ochs V *et al.* (1989) Molecular cloning, sequence analysis, and functional expression of a novel growth regulator, oncostatin M. *Mol Cell Biol* 9:2847–53

Martin P (1997) Wound healing–aiming for perfect skin repair. *Science* 276:75–81

Modur V, Feldhaus MJ, Weyrich AS, Jicha DL, Prescott SM, Zimmerman GA *et al.* (1997) Oncostatin M is a proinflammatory mediator. *In vivo* effects correlate with endothelial cell expression and inflammatory cytokines and adhesion molecules. *J Clin Invest* 100:158–68

Mosley B, De Imus C, Friend D, Boiani N, Thoma B, Park LS *et al.* (1996) Dual oncostatin M (OSM) receptors. Cloning and characterization of an alternative signaling subunit conferring OSM-specific receptor activation. *J Biol Chem* 271:32635–43

Repovic P, Fears CY, Gladson CL, Benveniste EN (2003) Oncostatin-M induction of vascular endothelial growth factor expression in astroglioma cells. *Oncogene* 22:8117–24

Rosner K, Ross C, Karlsmark T, Petersen AA, Gottrup F, Vejlsgard GL (1995) Immunohistochemical characterization of the cutaneous cellular infiltrate in different areas of chronic leg ulcers. *APMIS* 103:293–9

Singer AJ, Clark RAF (1999) Cutaneous wound healing. *N Engl J Med* 341:738–46

Stallmeyer B, Kämpfer H, Kolb N, Pfeilschifter J, Frank S (1999) The function of nitric oxide in wound repair: inhibition of inducible nitric oxide-synthase severely impairs wound reepithelialization. *J Invest Dermatol* 113:1090–8

Tanaka M, Miyajima A (2003) Oncostatin M, a multifunctional cytokine. *Rev Physiol Biochem Pharmacol* 149:39–52

Tanaka M, Hara T, Copeland NG, Gilbert DJ, Jenkins NA, Miyajima A (1999) Reconstitution of the functional mouse oncostatin M (OSM) receptor: molecular cloning of the mouse OSM receptor β subunit. *Blood* 93:804–15

Thakur ML, Li J, Chandy B, John EK, Gibbons G (1996) Transient neutropenia: neutrophil distribution and replacement. *J Nucl Med* 37:489–94

Vasse M, Pourtau J, Trochon V, Muraine M, Vannier JP, Lu H *et al.* (1999) Oncostatin M induces angiogenesis *in vitro* and *in vivo*. *Arterioscler Thromb Vasc Biol* 19:1835–42

Wallace PM, MacMaster JF, Rouleau KA, Brown JT, Loy JK, Donaldson KL *et al.* (1999) Regulation of inflammatory responses by oncostatin M. *J Immunol* 162:5547–55

Werner S, Grose R (2004) Regulation of wound healing by growth factors and cytokines. *Physiol Rev* 83:835–70

Wetzler C, Kämpfer H, Stallmeyer B, Pfeilschifter J, Frank S (2000) Large and sustained induction of chemokines during impaired wound healing in the genetically diabetic mouse: prolonged persistence of neutrophils and macrophages during the late phase of repair. *J Invest Dermatol* 115:245–53

Zarling JM, Shoyab M, Marquardt H, Hanson MB, Lioubin MN, Todaro GJ (1986) Oncostatin M: a growth regulator produced by differentiated histiocytic lymphoma cells. *Proc Natl Acad Sci USA* 83:9739–43